

Abstract:

Fram Strait is the primary pathway for sea ice export from the Arctic Ocean yet estimates of volume export are constrained by observations of ice thickness and drift. Using a new year-round CryoSat-2 ice thickness product we determine an average annual export of $1,712 \pm 452 \text{ km}^3$ from 2011-2022. 15% of the Arctic Oceans sea ice volume is exported annually, while 3.2% of the volume lost during the melt season is exported. Comparing high- and low-resolution ice drift products reveals the latter underestimate export by 30%. Comparing volume export between 82°N and 79°N reveals a high melt rate of 1 cm d^{-1} , reducing export by 53%. September sea ice volume declines by 286 km^3 for every 100 km^3 exported during summer, highlighting how export amplifies the ice-albedo feedback. Our estimates of volume export provide new insight into Fram Straits role as a sea ice sink and freshwater source.

Plain Language Summary:

Sea ice in the Arctic Ocean is either lost through melt or export. Fram Strait is the primary pathway for sea ice export, yet estimates of sea ice volume export are limited by the availability of ice thickness and drift data. Here we use a new year-round record of ice thickness from the satellite altimeter CryoSat-2 to refine the estimates of sea ice volume export from 2011 to 2022. Overall, we find that $1,712 \text{ km}^3$ or approximately 15% of the sea ice in the Arctic Ocean is exported annually. Calculating ice volume export at different locations reveals high melt rates in the area that thin the ice as it drifts south towards the north Atlantic Ocean. These estimates are not only key to understanding sea ice loss in the Arctic Ocean but also the supply of freshwater to the north Atlantic, where overturning is critical to the global climate.

56

57 1. Introduction:

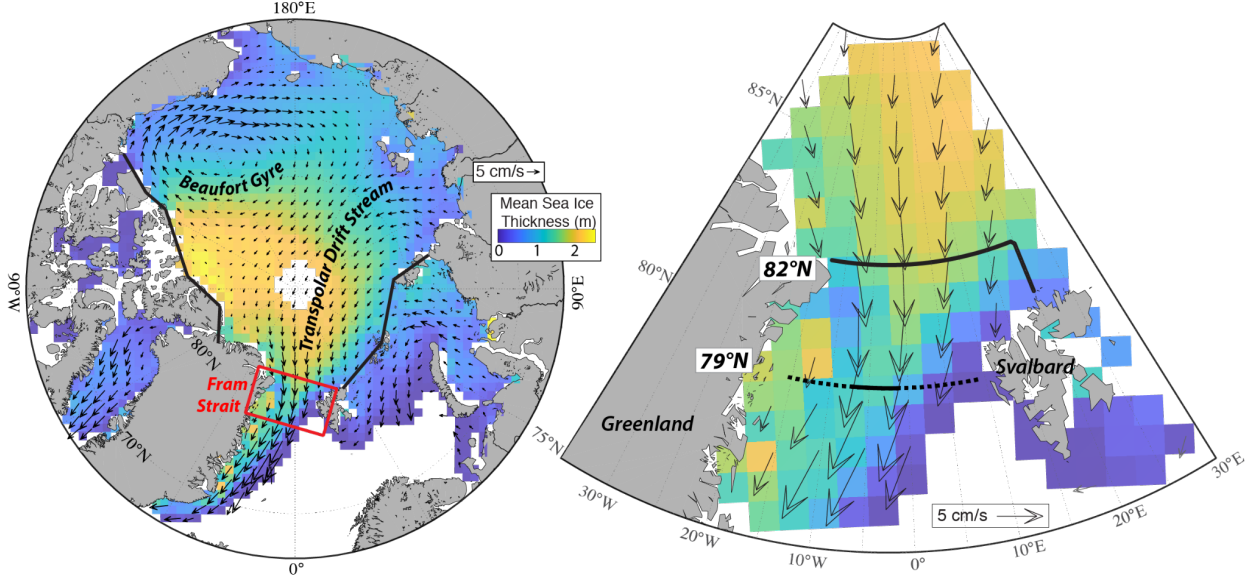
58 Fram Strait is the primary pathway for sea ice export from the Arctic Ocean. As a
59 result, it plays a significant role in both the ice mass balance of the Arctic Ocean and the
60 delivery of freshwater to the North Atlantic, where it impacts the Atlantic meridional
61 overturning circulation (Belkin et al., 1998; Ionita et al., 2016). Sea ice export through Fram
62 Strait removes approximately 10% of the sea ice area (Smedsrud et al., 2017) and 14% of
63 the sea ice volume in the Arctic Ocean annually (Spren et al., 2020), while also comprising
64 25% of the total freshwater delivered to the North Atlantic (Lique et al., 2009). Sea ice is
65 advected towards Fram Strait by the Transpolar Drift Stream (Figure 1A) while the sea level
66 pressure gradient across the Strait dictates wind speeds, which drive ice drift and therefore
67 ice flux through the Strait. This gradient drives a pronounced annual cycle in sea ice export
68 from a peak in March to a minimum in August (Smedsrud et al., 2017; Spren et al., 2020;
69 Vinje et al., 1998). On average, between 706,000 and 880,000 km² of sea ice is exported
70 through Fram Strait annually (Kwok, 2009; Smedsrud et al., 2017), however scaling this to
71 sea ice volume export has been limited by the availability of ice thickness data.

72 Historically, sea ice volume export has been examined along a flux gate at 79°N where
73 moored Upward Looking Sonars (ULS) have provided year-round observations of sea ice
74 thickness since 1990 (Figure 1B). Initial estimates in the 1990s varied between 2,218 and
75 2,850 km³ per year (Kwok, 2004; Kwok & Rothrock, 1999; Vinje et al., 1998). More recently,
76 Spren et al. (2020) determined an average annual volume export of 2,400 km³ from 1992-
77 2014 but found that a reduction in ice thickness (-15% per decade) has driven a reduction
78 in sea ice volume export (-27% per decade). In particular, the ULS have revealed a reduction
79 in the thickness of multi-year sea ice and presence of deformed ice in Fram Strait (Hansen et
80 al., 2013), while there was a particular shift towards younger thinner ice passing through
81 Fram Strait around 2007 (Babb et al., 2023; Sumata et al., 2023). Overall, annual average sea
82 ice volume export, as estimated from the ULS, has declined from 2,450 km³ in the 1990s, to
83 1,760 km³ in the 2000s and 1,390 km³ from 2010-2017, with a minimum of 590 km³ in 2018
84 (Sumata et al., 2022). The disparity between the long-term negative trend in volume export
85 and positive trend in area export (Smedsrud et al., 2017) highlights the importance of sea ice
86 thickness observations.

87 While the ULS provide high resolution observations of ice thickness year-round, they
88 are limited by their spatial coverage (7°W - 3°W; Figure 1B) and therefore require thickness
89 to be extrapolated across the gate, which leads to significant uncertainty in volume flux
90 estimates (i.e., 26% to 44%; Sumata et al., 2023). Conversely, satellite altimetry does not
91 offer the high temporal resolution of a ULS but does provide complete coverage across the
92 flux gate. Furthermore, the location of flux gates can be changed when using altimeters,
93 which provides insight into local changes to the ice pack (i.e., melt) and can offer greater
94 precision at higher latitudes where overpasses are more frequent (i.e., 82°N; Ricker et al.,
95 2018). The limitation with altimeters is that historically they only provided estimates of
96 thickness during winter (October to April), when the ice surface is cold. Using ICESat, Spreen
97 et al., (2009) estimated an average winter export of 1,564 km³ at 80°N from 2003-2008,
98 though this estimate relied on ULS to fill gaps between the two ICESat observing periods
99 (October-November and February-March). Using CryoSat-2, Ricker et al., (2018) estimated
100 an average winter export of 1,711 km³ at 82°N from 2010 to 2017. However, despite a
101 majority of sea ice export occurring during winter, there was a summer gap in satellite
102 estimates. Krumpfen et al., (2016) used sparse airborne ice thickness surveys to estimate an
103 average monthly export of 17 km³ during July and August. However, there remains a gap
104 during spring (May and June) when ice drift speeds remain modest, and a significant volume
105 of sea ice may still be exported.

106 Here we use new year-round estimates of ice thickness from CryoSat-2 (Landy et al.,
107 2022) in combination with a passive microwave ice drift product to close the annual record
108 of sea ice volume export through Fram Strait from 2010-2022. We further refine estimates
109 of volume export from 2016-2022 using high resolution observations of ice drift from
110 spaceborne synthetic aperture radar (SAR) imagery. We discuss the consistency between
111 published estimates of the volume flux, including the impact of selecting gates over the ULS
112 array at 79°N or further north. Finally, we consider the role of sea ice volume export through
113 Fram Strait in modulating the ice mass balance of the Arctic Ocean and the delivery of
114 freshwater to the North Atlantic.

115
116
117



118
 119 Figure 1: Mean fields of sea ice thickness and drift from 2010-2022 across the Arctic Ocean
 120 (left) and in the vicinity of Fram Strait (right) with the two gates at 82°N and 79°N presented.
 121 The Arctic Ocean for the ice mass balance analysis is defined by the black lines in the pan-
 122 Arctic map along with the Bering Strait and the chosen gate at Fram Strait. In the Fram Strait
 123 panel, the solid portion of the 79°N gate between 3° and 7°W is where the ULS are located.

124
 125 **2. Methods:**

126 Sea ice volume flux (F) through Fram Strait ($\text{km}^3 \text{d}^{-1}$) was calculated at 44 intervals
 127 (i) along the 82°N flux gate (Figure 1) previously used by Ricker et al., (2018). F was
 128 calculated using the following equation,

$$F_i = \sum_{i=1}^n (C_i H_i u_i \Delta x) \tag{1}$$

129
 130
 131 where C is fractional sea ice concentration, H is ice thickness (km), u is ice drift speed normal
 132 to the gate (km d^{-1}) and Δx is the interval (15 km). Positive values of F indicate sea ice export
 133 from the Arctic Ocean, while negative values indicate ice import into the Arctic Ocean. C , H
 134 and u were interpolated from gridded products to each interval at each time step. F is
 135 summed annually from October to September.

136
 137 Year-round fields of H from CryoSat-2 are provided at bimonthly intervals from
 138 October 2010 to July 2022 (Landy & Dawson, 2022). H is generally thinner in this product
 139 than the Alfred Wegener Institute (AWI) product used by Ricker et al., (2018) due to

140 differences in radar echo re-tracking (described in Landy et al. (2020)), and snow loading.
 141 The AWI product uses a modified Warren (1999) snow climatology, whereas Landy and
 142 Dawson (2022) uses the Lagrangian snow evolution scheme SnowModel-LG (Liston et al.,
 143 2020; Stroeve et al., 2020). Validating their product against the ULS in Fram Strait, Landy et
 144 al. (2022) found a mean bias of +11 cm.

145 For the full CryoSat-2 record, F was calculated from fields of sea ice concentration
 146 (Cavalieri et al., 1996; updated 2023) and motion (Tschudi et al., 2019; updated 2023)
 147 derived from spaceborne passive microwave sensors. These estimates are referred to as
 148 F_{PMW} . For comparison to previous studies, F_{PMW} was also calculated at 79°N. Sea ice area flux
 149 (km^2) was calculated by solving F_{PMW} without H .

150 F was also calculated from 2016-2022 using high spatiotemporal resolution ice drift
 151 data (i.e., ~1 day, 200 m) derived from a combination of spaceborne SAR imagery (i.e.,
 152 Sentinel-1, RADARSAT-2 and RADARSAT Constellation Mission) using the methodology of
 153 Komarov and Barber (2014) and ice concentration from daily ice charts from the National Ice
 154 Center (U.S. National Ice Center, 2023). These estimates are referred to as F_{SAR} . SAR resolves
 155 faster ice drift speeds than passive microwave drift products (Howell et al., 2022; Kwok et
 156 al., 1998; Smedsrud et al., 2017), which is important in Fram Strait where the fastest ice drift
 157 in the Arctic Ocean occurs (Figure 1).

158 Following Ricker et al., (2018) the uncertainty of F_{PMW} (σF_{PMW}) at each interval and
 159 time step, assuming uncorrelated errors between variables, is determined with the following
 160 equation,

$$161 \quad \sigma F_{PMW} = L \sqrt{(H C \sigma_u)^2 + (H \sigma_C u)^2 + (\sigma_H C u)^2} \quad (2)$$

162
 163 where, σH , σC and σu are the uncertainties in thickness, concentration and drift respectively,
 164 and L is the length of the interval. σC is set at 5% (Ricker et al., 2018). σH is taken from the
 165 CryoSat-2 product (Landy and Dawson, 2022) and has a mean of 0.32 m. σu is taken from
 166 Sumata et al., (2014) and set at 0.873 km d^{-1} during winter (October-April) and 1.123 km d^{-1}
 167 during summer (May-September). The monthly uncertainty at 82°N peaks in March and
 168 April at 60 km^3 per month and is 17 km^3 during August and September. The average annual
 169 uncertainty at 82°N and 79°N is 452 km^3 and 176 km^3 , which are equal to 26% and 21% of

170 the average annual fluxes, respectively. The uncertainty in F_{SAR} is lower as the error in SAR-
171 derived ice motion is estimated to be 0.43 km d^{-1} (Komarov & Barber, 2014).

172 Sea ice volume flux is scaled by 0.8 to estimate liquid freshwater flux relative to a
173 reference salinity of 34.8 (Haine et al., 2015). The contribution of snow to the freshwater flux
174 was calculated by replacing H in equation 1 with snow depth from SnowModel-LG and then
175 using snow density from the model to calculate the liquid equivalent (km^3).

176

177 **3. Results and Discussion:**

178 **3.1 Sea ice volume export at 82°N**

179 3.1.1 Sea ice volume export

180 The biweekly record of F_{PMW} through Fram Strait is presented in Figure 2A. On
181 average 72 km^3 of sea ice was exported biweekly, with a peak of 306 km^3 during late
182 February 2012. F_{PMW} was only positive (import) during 22 biweekly periods (8%), most of
183 which occurred between July and September, and all of which were below 20 km^3 and
184 therefore in the range of the monthly uncertainty. Similar to the annual record in sea ice area
185 export, the annual cycle in volume export shows a peak in March (305 km^3) and minimum in
186 August (19 km^3 ; Figure 2B; Table 1). The reduction during spring and summer is gradual, so
187 although F_{PMW} from July to September is very low (4% of the annual flux), F_{PMW} during May
188 and June, which have not been captured by previous altimeter or airborne estimates, make
189 a significant contribution ($\sim 15\%$) to the annual flux.

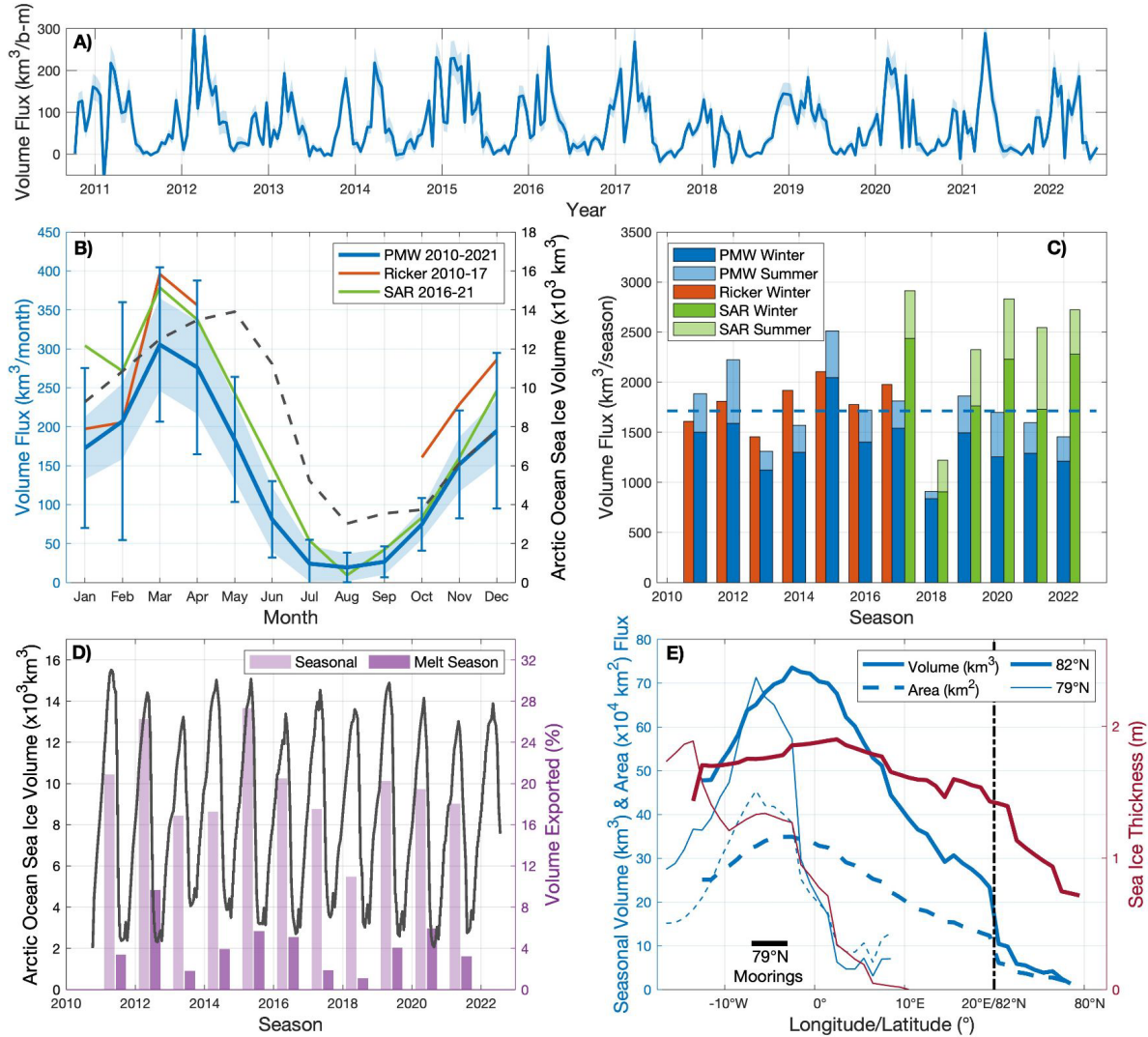
190 The monthly averages of F_{PMW} from winters 2010-2017 are 20% lower than those of
191 Ricker et al., (2018) (orange in Figure 2B), which is expected given that our estimates of ice
192 thickness are inherently thinner. Monthly averages of F_{PMW} from 2016-2022 are 27% lower
193 than F_{SAR} , which is expected given that SAR detects faster ice drift speeds. These disparities
194 highlight the importance of continuing to refine estimates of ice thickness and drift used to
195 calculate volume fluxes. Furthermore, it provides important context on the interpretation of
196 existing records of volume export derived from passive microwave drift products, which
197 may underestimate volume export by nearly one-third.

198 Over the full CryoSat-2 record, F_{PMW} gives an average annual export of $1,712 \text{ km}^3$
199 through Fram Strait with a peak of $2,512 \text{ km}^3$ in 2015 and minimum of 907 km^3 in 2018
200 (Figure 2C; Table 1). From 2016-2021, F_{SAR} gives an average annual export of $2,360 \text{ km}^3$, with

201 a peak of 2,914 km³ in 2017 and minimum of 1,219 km³ in 2018. Both datasets show a
202 minimum in 2018 due to anomalously low export from February to May (Table 1), but also
203 show a recovery in the years after, meaning 2018 did not provoke a step change in the
204 volume flux but was rather an anomalously low year. There is no apparent linear trend in
205 either F_{PMW} or F_{SAR} , although the records are too short for reliable climate signals to emerge.
206 For comparison, F_{PMW} and F_{SAR} through Fram Strait are nearly seven- and ten-times greater,
207 respectively, than the combined sea ice volume export through Nares Strait and the Canadian
208 Arctic Archipelago (Howell et al., 2023).

209 Seasonally, 80% (76% in F_{SAR}) of the volume export occurs during winter (October-
210 April) while the remaining 20% (24%) occurs during summer (May-September) and
211 represents the gap that year-round observations of ice thickness can fill. On average 360 km³
212 was exported during summer, with a peak of 633 km³ in 2012 and minimum of 71 km³ in
213 2018. Although the standard deviation of volume flux during winter is greater than summer
214 (305 vs 149 km³), the coefficient of variation for summer (44%) is double that for winter
215 (22%), indicating volume export is twice as variable during summer compared to winter.
216 Examining the contribution of concentration, drift, and thickness to the significant change in
217 variance between summer and winter we find that it is primarily due to the seasonal change
218 in ice drift. The coefficient of variation for ice drift increases from 79% in winter to 131% in
219 summer, compared to a negligible change in the contribution of concentration from 35% in
220 winter to 36% in summer, and a slight increase in the contribution of thickness from 55% in
221 winter to 63% in summer. Similarly, Ricker et al., (2018) found that a majority of the
222 variability in winter volume flux was due to variability in ice drift.

223



224
 225 Figure 2: Sea ice volume export at 82°N. A) bi-weekly record of F_{PMW} . B) Monthly cycle of
 226 F_{PMW} (2010-2022; blue), F_{SAR} (2016-2022; green) and F from Ricker et al., (2018; 2010-2017;
 227 orange) with the monthly cycle of sea ice volume in the Arctic Ocean (gray dashed). The
 228 shading in A) and B) represent the uncertainty in F_{PMW} . The error bars in B) represent the
 229 standard deviation in monthly F_{PMW} . C) Annual F_{PMW} from 2011-2022 decomposed by winter
 230 (October to April) and summer (May to September) compared against winter fluxes from
 231 Ricker et al., (2018; orange) and year-round F_{SAR} (green). The dashed line in C) shows the
 232 mean annual F_{PMW} . D) bi-weekly record of sea ice volume in the Arctic Ocean and the
 233 proportion (%) exported through Fram Strait annually and each melt season. E) Across-
 234 Strait profile of the mean annual sea ice area and volume fluxes per year, and the mean ice
 235 thickness at each interval (1° longitude at 82°N or 15 km). In E) the thick lines denote data
 236 for 82°N, the thin lines denote data for the 79°N, the vertical dashed line denotes the switch
 237 from a zonal to meridional gate along the 82°N gate and the thick black line shows the
 238 longitudinal span of the 79°N mooring array.

239 Table 1: Monthly sea ice volume flux (km³) through Fram Strait (82°N) from October 2010
 240 to July 2022. The monthly mean and annual sum are presented along their respective rows
 241 and columns. SAR estimates of sea ice volume flux are provided in brackets from February
 242 2016 to July 2022.

Month	Year													Mean
	2010	2011	2012	2013	2014	2015	2016	2017	2018	2019	2020	2021	2022	
Jan		295	54	75	32	151	85	358 (488)	206 (279)	244 (284)	118 (233)	152 (206)	300 (333)	173 (304)
Feb		-20	457	108	94	457	259 (42)	115 (266)	77 (17)	201 (193)	364 (723)	68 (78)	301 (582)	207 (271)
Mar		416	277	295	283	410	337 (194)	430 (474)	122 (125)	293 (400)	395 (740)	286 (399)	119 (318)	305 (379)
Apr		248	464	246	338	312	263 (93)	272 (412)	106 (117)	181 (234)	149 (269)	503 (727)	232 (510)	276 (337)
May		252	303	115	111	202	152 (130)	239 (251)	-19 (101)	205 (284)	206 (323)	222 (393)	212 (221)	183 (243)
Jun		101	149	41	40	164	54 (21)	47 (171)	70 (143)	102 (147)	153 (196)	36 (270)	16 (100)	81 (150)
Jul		19	95	27	1	63	39 (6)	-24 (36)	-9 (11)	5 (29)	34 (58)	23 (115)	17 (122)	24 (54)
Aug		3	34	8	62	8	48 (10)	10 (9)	4 (1)	13 (30)	6 (-1)	16 (6)		19 (9)
Sep		8	53	-3	56	30	29 (56)	-1 (11)	25 (58)	40 (73)	45 (27)	8 (28)		27 (42)
Oct	125	52	108	106	130	31	72 (101)	68 (58)	73 (149)	60 (47)	43 (39)	25 (104)		75 (83)
Nov	182	84	143	315	147	181	68 (166)	119 (110)	215 (201)	43 (74)	147 (104)	175 (306)		152 (160)
Dec	255	203	146	130	439	243	224 (530)	137 (199)	288 (300)	123 (141)	90 (180)	58 (126)		195 (246)
Sum		1884	2223	1310	1570	2512	1722	1811 (2914)	907 (1219)	1861 (2326)	1696 (2832)	1594 (2545)	1455 (2722)	

243

244 3.1.2 Sea ice volume export and the Arctic Ocean ice mass balance

245 Comparing the biweekly record of F_{PMW} and total sea ice volume within the Arctic
 246 Ocean (Figure 2D - boundaries in Figure 1A) we quantify the contribution of volume export
 247 through Fram Strait to the sea ice mass balance of the Arctic Ocean. Between 2011 and 2022,
 248 an average of 14.6% of the sea ice volume in the Arctic Ocean was exported through Fram
 249 Strait annually (Figure 2E). This is similar to the 14% reported by Spreen et al., (2020) using
 250 ULS data for export and PIOMAS for sea ice volume from 1992-2014 and implies that this
 251 proportion has been relatively stable over the last 30 years. This might be expected given
 252 that both sea ice volume in the Arctic Ocean and export through Fram Strait have declined at
 253 respective rates of -15% per decade (Kwok, 2018) and -27% per decade (Spreen et al., 2020).
 254 The proportion peaked at 21.8% in 2012, when volume export was the second highest of the
 255 study period and fell to a minimum of 7.4% in 2018. For comparison, over the same period
 256 11% of the sea ice area in the Arctic Ocean was exported through Fram Strait annually,
 257 highlighting the higher-than-average thickness of ice passing through Fram Strait.

258 During summer, sea ice volume export through Fram Strait explained only 3.2% of
259 the average 10,400 km³ of sea ice lost from the Arctic Ocean between May and September
260 (Figure 2B). For comparison, 5% of the reduction in sea ice area was due to export. Fram
261 Strait has a lower impact on summer volume loss than area loss because volume and area
262 are both lost from ice that melts out completely, while volume is also lost from ice that
263 persists through September. The contribution of sea ice export to the loss of sea ice during
264 summer peaked at 5.5% in 2012, when summer volume export peaked and contributed to
265 the record sea ice minimum (Zhang et al., 2013), and was below 1% in 2018, when volume
266 export was anomalously low (77 km³). Interestingly, summer volume export was only 2%
267 during 2013 and 2017, which were both years of recovery following years of record sea ice
268 loss.

269 Overall, summer sea ice volume export is found to be significantly correlated with
270 September sea ice volume in the Arctic Ocean ($r = -0.68$, $p < 0.05$), while the relationship
271 between annual export and September volume was not significant. Based on this
272 relationship, September sea ice volume declines by 286 km³ for every 100 km³ exported
273 during summer, the relationship is not one-to-one as export amplifies other feedbacks that
274 in turn drive ice melt (i.e., ice-albedo feedback). Given the high degree of uncertainty in
275 volume flux estimates, we test the robustness of this relationship by running 1000 iterations
276 with random uncertainties drawn from a normal distribution of the summer flux uncertainty
277 ($\overline{\sigma F_S} = 148 \text{ km}^3$) applied to summer estimates of volume export. The relationship
278 remained significant in 80% of the iterations, suggesting a robust negative relationship
279 between summer volume export and September volume. A similar test with the annual
280 volume export and September sea ice volume resulted in a significant negative relationship
281 in only 2.5% of the iterations, supporting our finding of no relationship between the two.
282 This implies that years with higher winter sea ice export do not precondition the Arctic's sea
283 ice cover in spring for higher-than-normal melt and anomalously low September sea ice
284 volume. High winter export may be offset by an enhanced negative thin ice-thermodynamic
285 growth feedback (Stroeve et al., 2018).

286

287 3.1.3 Across Strait profiles

288 Satellite altimeters offer unique insight into the across-strait profile in ice thickness
289 not captured by the ULS. Figure 2E shows the average across strait profiles in ice thickness,
290 and the annual sea ice area and volume fluxes at 82°N and 79°N. At 82°N thickness is
291 approximately 1.7 m near Greenland with a peak of 1.9 m around 2°E, a reduction towards
292 1.5 m across the zonal gate before falling below 0.7 m along the meridional gate. Sea ice area
293 flux between 2010 and 2022 peaked at 3°W and fell off quickly across the zonal gate with
294 minimal export across the meridional gate as the normal component of the ice drift in this
295 area is minimal. As the compound of the ice thickness and area flux profiles, the sea ice
296 volume flux peaked at 3°W and declined across the zonal gate with very little volume being
297 exported across the meridional gate. Export peaks in this area because of the East Greenland
298 Current driving greater ice drift speeds (Ricker et al., 2018; Figure 1).

299

300 **3.2 Comparison between 82°N and 79°N and previous estimates.**

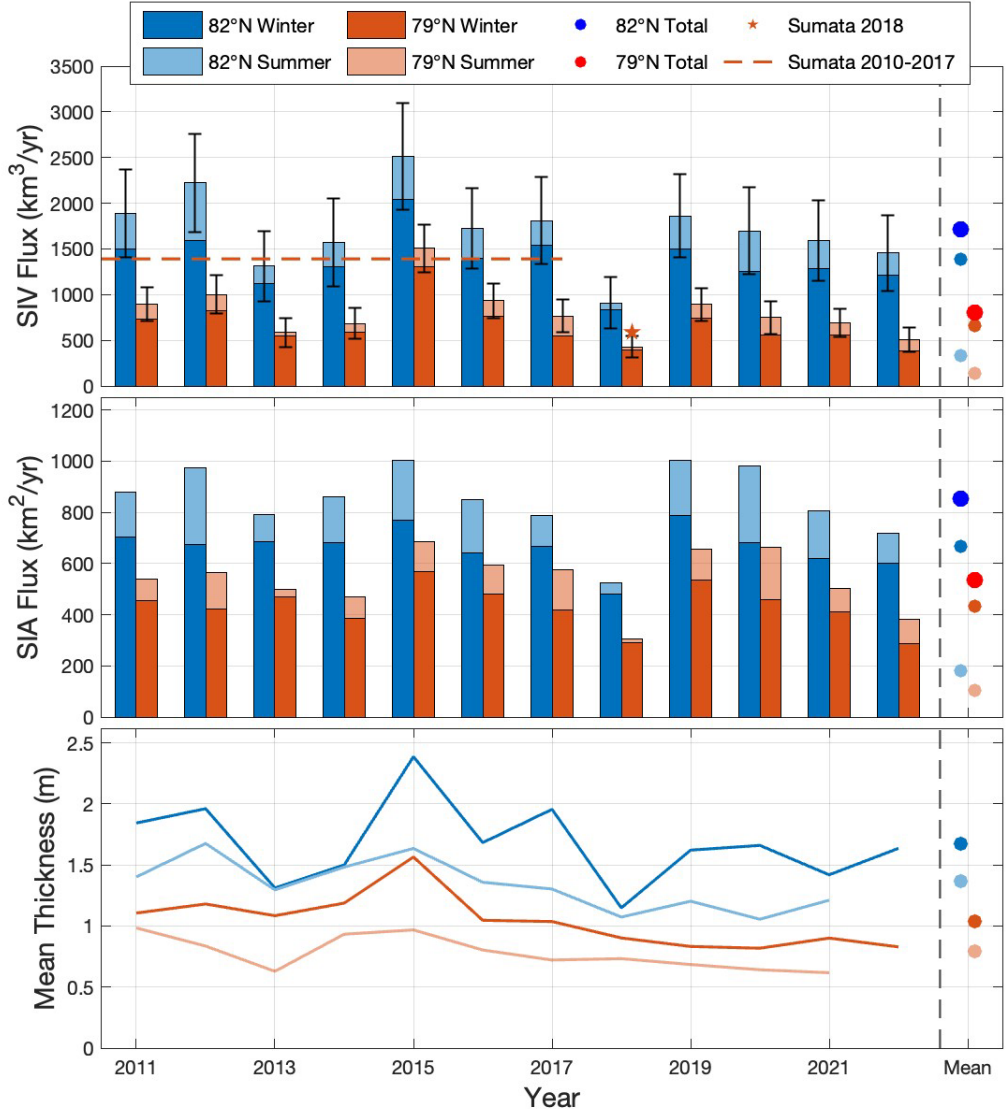
301 F_{PMW} declined by 52% between 82°N and 79°N, with a slightly greater decrease during
302 summer (58%) than winter (51%) (Figure 3). Reductions in both sea ice area flux (-36%)
303 and thickness (-38%) drive the overall reduction in volume flux. The reduction in area flux
304 is greater than the 10% reduction between 82°N and 79°N reported by Spreen et al., (2020),
305 though their gates were oriented differently, and their study extended back to 1992, meaning
306 that our observations could highlight a recent increase in the amount of sea ice area lost
307 between these two gates. The reduction in area flux is primarily the result of a contraction
308 of sea ice towards the Greenlandic coast (Figure 1B; 2E), however, this contraction does not
309 represent ice convergence, as the ice thickness also declines between the gates. On average
310 ice thickness declined by 0.20 m per degree-latitude between the gates, which was fairly
311 consistent between winter (-0.20 m) and summer (-0.18 m) and agrees with the thinning
312 rate of 0.19 m per degree-latitude observed during summer by Krumpfen et al., (2016). Given
313 that the gates are separated by 333 km and the average drift speed over the two gates
314 throughout the CryoSat-2 period is 5.6 km d⁻¹, it takes an average of 59 days for the ice to
315 drift from 82°N to 79°N. With an average thinning of 0.60 m between the gates over the full
316 CryoSat-2 period, this equates to nearly 1 cm of melt per day throughout the year as the ice
317 drifts between the two gates. Similarly, Sumata et al., (Duarte et al., 2020; Provost et al., 2017;
318 Sirevaag & Fer, 2009; 2022) estimated high melt rates between 0.43 and 2.2 cm d⁻¹

319 immediately upstream of their flux gate at 79°N using altimetry-based estimates of ice
320 thickness along backward trajectories of the ice passing by the ULS. These high melt rates
321 highlight the influence of warm Atlantic water in Fram Strait driving rapid ice melt in the
322 vicinity of Fram Strait (i.e., Duarte et al., 2020; Sirevaag and Fer, 2009; Provost et al., 2017).

323 Our estimates of F_{PMW} at 79°N are routinely lower than previous estimates at this gate
324 (i.e., Kwok & Rothrock, 1999; Spreen et al., 2020; Sumata et al., 2022; Vinje et al., 1998). The
325 difference with historic estimates from the 1990s is primarily due to the transition towards
326 a younger, thinner ice pack passing through Fram Strait (i.e., Babb et al., 2023; Sumata et al.,
327 2023). However, focusing on the period from 2010-2018, our estimates are 33% less than
328 those from Sumata et al., (2022). This difference is likely to be caused by the high degree of
329 uncertainty associated with extrapolating the across-Strait thickness profile from ULS that
330 cover only 85 of the 588 km across the 79°N gate, which may overestimate ice thickness
331 (Figure 2E). It may also be caused by CryoSat-2 underestimating the thickness of very thick
332 and rough ice floes in Fram Strait; however, CryoSat-2 overestimated the ULS ice thickness
333 by 11 cm when the observations were directly compared (Landy et al., 2022).

334

335



336
 337 Figure 3: Annual sea ice volume (A) and area (B) fluxes and the mean annual ice thickness
 338 (C) for the 82°N and 79°N flux gates. The mean for the winter, summer and annual fluxes,
 339 along with the mean winter and summer thicknesses are presented on the far right of each
 340 plot. The error bars in A) represent the annual uncertainty in F_{PMW} at 82°N and 79°N.
 341 Estimates of sea ice volume flux at 79°N from Sumata et al., (2022) are provided in Panel A.
 342

343 **3.3 Freshwater Export Through Fram Strait.**

344 In addition to serving as a sink for the ice mass balance of the Arctic Ocean, sea ice
 345 export through Fram Strait provides a large source of freshwater to the North Atlantic. For
 346 the sake of comparing the solid (sea ice and snow) and liquid components of the freshwater
 347 export through Fram Strait, we focus on the flux gate at 79°N where the moorings provide a

348 long-term record of liquid freshwater export (Rabe et al., 2013; de Steur et al., 2009). Our
349 estimates of F_{PMW} are equal to an annual average freshwater flux of 664 km³ with an
350 additional 17 km³ of freshwater from snow, for a total solid freshwater flux of 681 km³ yr⁻¹
351 during the 2010s. This is considerably lower than previous freshwater budgets have
352 estimated (2,300 km³ yr⁻¹ Serreze et al., 2006; 1900 km³ yr⁻¹ Haine et al., 2015), because
353 these estimates have been based on historic observations of a thicker ice pack and were
354 subject to the increased uncertainty of extrapolating ULS observations across the full 79°N
355 gate (i.e., Vinje et al., 1998). The solid freshwater flux is only 21% of the liquid freshwater
356 flux observed at the moorings (3,160 km³; Rabe et al., 2013), though based on the increased
357 melt rates between gates, we can estimate that up to 21% of this liquid freshwater flux is
358 released as ice melts immediately upstream of 79°N. Furthermore, our estimate of solid
359 freshwater flux through Fram Strait is double the estimated solid freshwater flux through
360 Davis Strait (331 km³ yr⁻¹; Curry et al., 2014), which is the other pathway for sea ice export
361 into the North Atlantic. Together Fram and Davis Straits provide approximately 1,012 km³
362 yr⁻¹ of freshwater to the North Atlantic.

363 Given that there is no long-term trend in liquid freshwater flux through Fram Strait
364 (Rabe et al., 2013), we suggest that the reduction in sea ice volume export (Spren et al.,
365 2020; Sumata et al., 2022) has led to an overall reduction in the total annual delivery of
366 freshwater to the North Atlantic through Fram Strait. The magnitude of the total freshwater
367 flux is projected to change under a warming climate, with reduced sea ice export but
368 potentially enhanced liquid freshwater export through Fram Strait because of enhanced
369 freshwater storage within the Arctic Ocean (Haine et al., 2015; Holland et al., 2007).

370

371 **Conclusions:**

372 A new year-round record of sea ice thickness from CryoSat-2 is used to complete the
373 annual record of satellite-based estimates of Arctic sea ice volume export through Fram
374 Strait. Using a passive microwave ice drift product over the full CryoSat-2 period (2010-
375 2022), we find an average annual (October to September) export of 1,712 km³ (± 452 km³)
376 with 80% occurring during winter (October to April) and 20% during summer (May to
377 September), the latter of which has not previously been captured by satellite altimeter-based
378 studies. However, compared to volume export derived from high resolution observations of

379 ice drift from SAR imagery, we find that passive microwave estimates underestimate volume
380 export by nearly one-third, suggesting many previous records of volume export have
381 underestimated the magnitude of sea ice export.

382 In terms of the ice mass balance of the Arctic Ocean, 14.6% of the Arctic Oceans sea
383 ice volume is exported through Fram Strait annually, while 3.2% of the sea ice volume lost
384 during the melt season is through export. We find a robust significant negative relationship
385 between summer sea ice volume export and September sea ice volume in the Arctic Ocean,
386 which declines by 286 km³ for every 100 km³ exported. Comparing sea ice volume export
387 between the northerly gate at 82°N and the historic flux gate at 79°N, we find a 52%
388 reduction. This highlights high melt rates in the vicinity of Fram Strait, with a year-round
389 thinning of approximately 1 cm d⁻¹ during the 60 days that it takes for ice to drift between
390 the gates. Our estimates of volume export across 79°N are three to four times below previous
391 estimates based on historic sea ice thickness observations, which highlights the long-term
392 negative trend in ice thickness and therefore volume export through Fram Strait. We suggest
393 the reduction in sea ice export is reducing the overall freshwater flux to the North Atlantic.
394 Our estimated freshwater volume flux through 79°N is only 21% of the observed liquid
395 freshwater flux across the same gate, though our results show that the same volume of
396 freshwater may have been released through ice melt immediately upstream of the flux gate.
397 Overall, we provide new estimates of sea ice volume flux through Fram Strait and its
398 influence on the Arctic Oceans ice mass balance, its role as a source for freshwater to the
399 North Atlantic, and importantly the uncertainty associated with previous estimates of this
400 critical term.

401

Acknowledgements:

403 This work is a contribution to the Canada Excellence Research Chair (CERC) in Arctic Ice,
404 Freshwater Marine Coupling and Climate Change held by D. Dahl-Jensen at the University of
405 Manitoba. D. Babb and S. Kirillov are supported by the CERC. D. Babb, J. Ehn and J. Stroeve
406 would like to acknowledge financial support from the Natural Sciences and Engineering
407 Research Council of Canada (NSERC). J. Landy acknowledges support from the Research
408 Council of Norway (RCN) INTERAAC project under grant #328957, from the ERC project
409 SI/3D under grant #101077496, and from the Fram Centre program for Sustainable
410 Development of the Arctic Ocean (SUDARCO) under grant #2551323. J. Stroeve is supported
411 by the Canada 150 Research Chair Program.

412

Data Availability Statement

414 The year-round record of sea ice thickness from CryoSat-2 is available from Landy and
415 Dawson (2022). Daily fields of sea ice concentration and motion as observed by passive
416 microwave satellites are available from Cavalieri et al., (1996) and Tschudi et al., (2019),
417 respectively. We are in the process of packaging up the SAR ice motion data and adding it to
418 the following ECCC repository [https://crd-data-donnees-
rdc.ec.gc.ca/CPS/products/IceFlux/](https://crd-data-donnees-
419 rdc.ec.gc.ca/CPS/products/IceFlux/).

420 **References:**

- 421 Babb, D. G., Galley, R. J., Kirillov, S., Landy, J. C., Howell, S. E. L., Stroeve, J. C., et al. (2023).
 422 The Stepwise Reduction of Multiyear Sea Ice Area in the Arctic Ocean Since 1980. *Journal*
 423 *of Geophysical Research: Oceans*, 128(10), 1–19. <https://doi.org/10.1029/2023JC020157>
- 424 Belkin, I. M., Levitus, S., Antonov, J., & Malmberg, S.-A. (1998). “Great Salinity Anomalies” in
 425 the North Atlantic. *Progress in Oceanography* (Vol. 41).
- 426 Cavalieri, D. J., Parkinson, C. L., Gloersen, P., & Zwally, H. J. (1996). *Sea Ice Concentrations*
 427 *from Nimbus-7 SMMR and DMSP SSM/I-SSMIS Passive Microwave Data*. Boulder,
 428 Colorado, USA.
- 429 Curry, B., Lee, C. M., Petrie, B., Moritz, R. E., & Kwok, R. (2014). Multiyear Volume, Liquid
 430 Freshwater, and Sea Ice Transports through Davis Strait, 2004–10. *Journal of Physical*
 431 *Oceanography*, 44(4), 1244–1266. <https://doi.org/https://doi.org/10.1175/JPO-D-13-0177.1>
- 432 Duarte, P., Sundfjord, A., Meyer, A., Hudson, S. R., Spreen, G., & Smedsrud, L. H. (2020).
 433 Warm Atlantic Water Explains Observed Sea Ice Melt Rates North of Svalbard. *Journal of*
 434 *Geophysical Research: Oceans*, 125(8). <https://doi.org/10.1029/2019JC015662>
- 435 Haine, T. W. N., Curry, B., Gerdes, R., Hansen, E., Karcher, M., Lee, C., et al. (2015, February
 436 1). Arctic freshwater export: Status, mechanisms, and prospects. *Global and Planetary*
 437 *Change*. Elsevier B.V. <https://doi.org/10.1016/j.gloplacha.2014.11.013>
- 438 Hansen, E., Gerland, S., Granskog, M. A., Pavlova, O., Renner, A. H. H., Haapala, J., et al.
 439 (2013). Thinning of Arctic sea ice observed in Fram Strait: 1990–2011. *Journal of*
 440 *Geophysical Research: Oceans*, 118(10), 5202–5221. <https://doi.org/10.1002/jgrc.20393>
- 441 Holland, M. M., Finnis, J., Barrett, A. P., & Serreze, M. C. (2007). Projected changes in Arctic
 442 Ocean freshwater budgets. *Journal of Geophysical Research: Biogeosciences*, 112(4).
 443 <https://doi.org/10.1029/2006JG000354>
- 444 Howell, S. E.L., Babb, D. G., Landy, J. C., Moore, G. W. K., Montpetit, B., & Brady, M. (2023). A
 445 Comparison of Arctic Ocean Sea Ice Export Between Nares Strait and the Canadian Arctic
 446 Archipelago. *Journal of Geophysical Research: Oceans*, 128(4).
 447 <https://doi.org/10.1029/2023JC019687>
- 448 Howell, Stephen E.L., Brady, M., & Komarov, A. S. (2022). Generating large-scale sea ice
 449 motion from Sentinel-1 and the RADARSAT Constellation Mission using the Environment
 450 and Climate Change Canada automated sea ice tracking system. *Cryosphere*, 16(3),
 451 1125–1139. <https://doi.org/10.5194/tc-16-1125-2022>
- 452 Ionita, M., Scholz, P., Lohmann, G., Dima, M., & Prange, M. (2016). Linkages between
 453 atmospheric blocking, sea ice export through Fram Strait and the Atlantic Meridional
 454 Overturning Circulation. *Scientific Reports*, 6. <https://doi.org/10.1038/srep32881>
- 455 Komarov, A. S., & Barber, D. G. (2014). Sea Ice Motion Tracking From Sequential Dual-
 456 Polarization RADARSAT-2 Images. *IEEE Transactions on Geoscience and Remote*
 457 *Sensing*, 52(1), 121–136. <https://doi.org/10.1109/TGRS.2012.2236845>
- 458 Krumpfen, T., Gerdes, R., Haas, C., Hendricks, S., Herber, A., Selyuzhenok, V., et al. (2016).
 459 Recent summer sea ice thickness surveys in Fram Strait and associated ice volume fluxes.
 460 *Cryosphere*, 10(2), 523–534. <https://doi.org/10.5194/tc-10-523-2016>
- 461 Kwok, R. (2004). Fram Strait sea ice outflow. *Journal of Geophysical Research*, 109(C1),
 462 C01009. <https://doi.org/10.1029/2003JC001785>

- 463 Kwok, R. (2009). Outflow of Arctic Ocean sea ice into the Greenland and Barent Seas: 1979-
464 2007. *Journal of Climate*, 22(9), 2438–2457. <https://doi.org/10.1175/2008JCLI2819.1>
- 465 Kwok, R. (2018). Arctic sea ice thickness, volume, and multiyear ice coverage: losses and
466 coupled variability (1958 – 2018). *Environmental Research Letters*, 13(10), 105005.
467 <https://doi.org/10.1088/1748-9326/aae3ec>
- 468 Kwok, R., & Rothrock, D. A. (1999). Variability of Fram Strait ice flux and North Atlantic
469 Oscillation. *Journal of Geophysical Research*, 104(C3), 5177–5189.
- 470 Kwok, R., Schweiger, A., Rothrock, D. A., Pang, S., & Kottmeier, C. (1998). Sea ice motion from
471 satellite passive microwave imagery assessed with ERS SAR and buoy positions. *Journal*
472 *of Geophysical Research*, 103(C4), 8191–8214. <https://doi.org/10.1029/97JC03334>
- 473 Landy, J., & Dawson, G. (2022). Year-round Arctic sea ice thickness from CryoSat-2 Baseline-D
474 Level 1b observations 2010-2020 (Version 1.0) [Data set].
- 475 Landy, J. C., Petty, A. A., Tsamados, M., & Stroeve, J. C. (2020). Sea Ice Roughness
476 Overlooked as a Key Source of Uncertainty in CryoSat-2 Ice Freeboard Retrievals. *Journal*
477 *of Geophysical Research: Oceans*, 125(5), 1–18. <https://doi.org/10.1029/2019JC015820>
- 478 Landy, J. C., Dawson, G. J., Tsamados, M., Bushuk, M., Stroeve, J. C., Howell, S. E. L., et al.
479 (2022). A year-round satellite sea-ice thickness record from CryoSat-2. *Nature*, 609(7927),
480 517–522. <https://doi.org/10.1038/s41586-022-05058-5>
- 481 Lique, C., Treguier, A. M., Scheinert, M., & Penduff, T. (2009). A model-based study of ice and
482 freshwater transport variability along both sides of Greenland. *Climate Dynamics*, 33(5),
483 685–705. <https://doi.org/10.1007/s00382-008-0510-7>
- 484 Liston, G. E., Itkin, P., Stroeve, J., Tschudi, M., Stewart, J. S., Pedersen, S. H., et al. (2020). A
485 Lagrangian Snow-Evolution System for Sea-Ice Applications (SnowModel-LG): Part I—
486 Model Description. *Journal of Geophysical Research: Oceans*, 125(10).
487 <https://doi.org/10.1029/2019JC015913>
- 488 Provost, C., Sennéchaël, N., Miguet, J., Itkin, P., Rösel, A., Koenig, Z., et al. (2017).
489 Observations of flooding and snow-ice formation in a thinner Arctic sea-ice regime during
490 the N-ICE2015 campaign: Influence of basal ice melt and storms. *Journal of Geophysical*
491 *Research: Oceans*, 122(9), 7115–7134. <https://doi.org/10.1002/2016JC012011>
- 492 Rabe, B., Dodd, P. A., Hansen, E., Falck, E., Schauer, U., MacKensen, A., et al. (2013). Liquid
493 export of Arctic freshwater components through the Fram Strait 1998–2011. *Ocean*
494 *Science*, 9(1), 91–109. <https://doi.org/10.5194/os-9-91-2013>
- 495 Ricker, R., Girard-Ardhuin, F., Krumpfen, T., & Lique, C. (2018). Satellite-derived sea ice export
496 and its impact on Arctic ice mass balance. *The Cryosphere*, 12(9), 3017–3032.
497 <https://doi.org/10.5194/tc-12-3017-2018>
- 498 Serreze, M. C., Barrett, A. P., Slater, A. G., Woodgate, R. A., Aagaard, K., Lammers, R. B., et
499 al. (2006). The large-scale freshwater cycle of the Arctic. *Journal of Geophysical Research:*
500 *Oceans*, 111(11), 1–19. <https://doi.org/10.1029/2005JC003424>
- 501 Sirevaag, A., & Fer, I. (2009). Early spring oceanic heat fluxes and mixing observed from drift
502 stations north of Svalbard. *Journal of Physical Oceanography*, 39(12), 3049–3069.
503 <https://doi.org/10.1175/2009JPO4172.1>
- 504 Smedsrud, L. H., Halvorsen, M. H., Stroeve, J. C., Zhang, R., & Kloster, K. (2017). Fram Strait
505 sea ice export variability and September Arctic sea ice extent over the last 80 years.
506 *Cryosphere*, 11(1), 65–79. <https://doi.org/10.5194/tc-11-65-2017>

- 507 Spreen, G., Kern, S., Stammer, D., & Hansen, E. (2009). Fram Strait sea ice volume export
 508 estimated between 2003 and 2008 from satellite data. *Geophysical Research Letters*,
 509 36(19), 1–6. <https://doi.org/10.1029/2009GL039591>
- 510 Spreen, G., de Steur, L., Divine, D., Gerland, S., Hansen, E., & Kwok, R. (2020). Arctic Sea Ice
 511 Volume Export Through Fram Strait From 1992 to 2014. *Journal of Geophysical Research:
 512 Oceans*, 125(6). <https://doi.org/10.1029/2019JC016039>
- 513 de Steur, L., Hansen, E., Gerdes, R., Karcher, M., Fahrbach, E., & Holfort, J. (2009).
 514 Freshwater fluxes in the East Greenland Current: A decade of observations. *Geophysical
 515 Research Letters*, 36(23), 1–5. <https://doi.org/10.1029/2009GL041278>
- 516 Stroeve, J., Liston, G. E., Buzzard, S., Zhou, L., Mallett, R., Barrett, A., et al. (2020). A
 517 Lagrangian Snow Evolution System for Sea Ice Applications (SnowModel-LG): Part II—
 518 Analyses. *Journal of Geophysical Research: Oceans*, 125(10).
 519 <https://doi.org/10.1029/2019JC015900>
- 520 Stroeve, J. C., Schroder, D., Tsamados, M., & Feltham, D. (2018). Warm winter, thin ice?
 521 *Cryosphere*, 12(5), 1791–1809. <https://doi.org/10.5194/tc-12-1791-2018>
- 522 Sumata, H., Lavergne, T., Girard-Ardhuin, F., Kimura, N., Tschudi, M. A., Kauker, F., et al.
 523 (2014). An intercomparison of Arctic ice drift products to deduce uncertainty estimates.
 524 *Journal of Geophysical Research: Oceans*, 119, 4887–4921.
 525 <https://doi.org/10.1002/2013JC009724>
- 526 Sumata, H., de Steur, L., Gerland, S., Divine, D. V., & Pavlova, O. (2022). Unprecedented
 527 decline of Arctic sea ice outflow in 2018. *Nature Communications*, 13(1).
 528 <https://doi.org/10.1038/s41467-022-29470-7>
- 529 Sumata, H., de Steur, L., Divine, D. V., Granskog, M. A., & Gerland, S. (2023). Regime shift in
 530 Arctic Ocean sea ice thickness. *Nature*, 615(7952), 443–449.
 531 <https://doi.org/10.1038/s41586-022-05686-x>
- 532 Tschudi, M. A., Meier, W. N., Stewart, J. S., Fowler, C., & Maslanik, J. A. (2019). *Polar
 533 Pathfinder Daily 25 km EASE-Grid Sea Ice Motion Vectors, Version 4*. Boulder, Colorado,
 534 USA. <https://doi.org/https://doi.org/10.5067/INAWUWO7QH7B>
- 535 Vinje, T., Nordlund, N., & Kvambekk, A. (1998). Monitoring ice thickness in Fram Strait. *Journal
 536 of Geophysical Research*, 103(C5), 10,437-10,449.
- 537 Warren, S. G., Rigor, I. G., Untersteiner, N., Radionov, V. F., Bryazgin, N. N., Aleksandrov, Y. I.,
 538 & Colony, R. L. (1999). Snow Depth on Arctic Sea Ice. *Journal of Climate*, 12, 1814–1829.
 539 [https://doi.org/10.1175%2F1520-
 540 0442%281999%29012%3C1814%3ASDOASI%3E2.0.CO%3B2](https://doi.org/10.1175%2F1520-0442%281999%29012%3C1814%3ASDOASI%3E2.0.CO%3B2)
- 541 Zhang, J., Lindsay, R., Schweiger, A., & Steele, M. (2013). The impact of an intense summer
 542 cyclone on 2012 Arctic sea ice retreat. *Geophysical Research Letters*, 40(4), 720–726.
 543 <https://doi.org/10.1002/grl.50190>
- 544
- 545